Postbuckling of Shear Deformable Composite Flat Panels Taking Into Account Geometrical Imperfections

L. Librescu*
Virginia Polytechnic Institute and State University, Blacksburg, Virginia 24061
and
M. Stein†
NASA Langley Research Center, Hampton, Virginia 23665

The postbuckling behavior of composite flat panels subjected to uniaxial/biaxial compressive loads is investigated. To this end a refined geometrically nonlinear theory of composite plates is developed. The effects played by transverse shear deformation, initial geometric imperfections, the character of the in-plane boundary conditions and lamination are studied and a series of pertinent conclusions are outlined. Throughout the paper, the results obtained within the transverse shear deformable plate model are compared with their classical counterparts and conclusions related to their range of applicability are presented.

Introduction

LAMINATED composite structures are being increasingly used in the aeronautical and aerospace constructions. Employment in their design of new material systems that exhibit exotic properties such as high anisotropy ratios requires a better understanding of their behavior. In order to be able to exploit the efficiency of composite structures, their postbuckling behavior needs to be considered. Such analyses have been done, mainly for structures modeled within the classical Kirchhoff hypothesis. The postbuckling strength exhibited by the metallic panels has permitted design of the conventional aircraft structural elements as to operate within the postbuckling range.

Moreover, it has been known for many years that small initial imperfections in some structures can produce large reductions in their static buckling strength. Research on the behavior of flat (and curved) panels[1] indicates that small initial deviations from perfect geometry could have a significant influence on both the buckling and postbuckling behavior. The great prospects emerging from the use of composite material structures in the design of the actual and future generations of aeronautical/aerospace vehicles, of deep submerged vessels, of naval constructions, etc., stimulate an obvious interest for the analysis of the postbuckling behavior of composite structures exhibiting small geometrical deviations from their initial flat configuration.

Moreover, as is well known,[2] the composite structures in contrast to their metallic counterparts exhibit high flexibilities in transverse shear. Since the research on postbuckling behavior of shear deformable composite imperfect structures appears to be somewhat scarce (see the survey papers[3-6] and the monographs,[7-9]) the present paper will be devoted to this topic. In contrast to the paper[10] where the principal goals were to determine through numerical and experimental simulations the postbuckling response and failure initiation of shear deformable composite panels, here, the main goal is to assess the role played by transverse shear flexibility and the initial geometric imperfections on their postbuckling behavior.

General Considerations

The case of a flat plate of uniform thickness h, symmetrically laminated of $2m + 1$ ($m = 1, 2 . . .$) elastic transversely isotropic layers (see Fig. 1), is considered. It is assumed that the planes of isotropy of each layer material are parallel at each point to the reference plane of the composite panel (selected to coincide with the midplane of the midlayer). Because of its special thermomechanical properties[11,12] (the transversely isotropic material is specifically suited for the thermal protection of aerospace vehicles and is useful in the design of missile and re-entry vehicle structures) and its high flexibility in transverse shear (manifested by large ratios of E/G' where E and G' denote the in-plane Young's modulus and transverse shear modulus, respectively), the consideration of this case in our analysis is both of theoretical and practical importance.

It is also assumed that the layers are in perfect bond, implying that no slip between two contiguous layers may occur.

The points of the three-dimensional (3-D) space of the plate will be referred to a set of rectangular Cartesian normal system of coordinates x_i, where x_α ($\alpha = 1, 2$) denote the in-plane coordinates, while x_3 denotes the normal one to the plane $x_3 = 0$ (defining the reference plane). For this case,
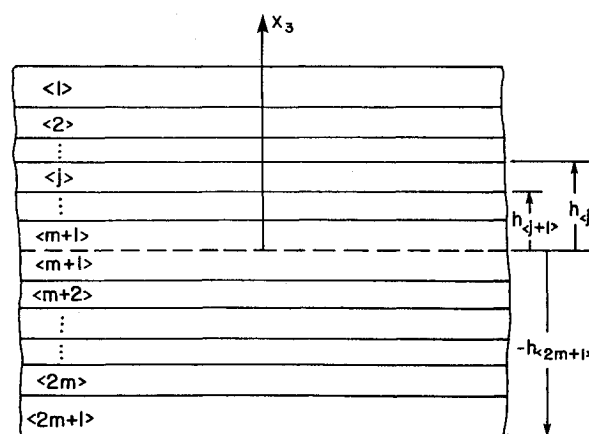
Fig. 1 Geometry of the cross section of the laminate.

the following relations for the components of the metric tensor hold valid:

$$g_{\alpha\beta} = a_{\alpha\beta} \equiv \delta_{\alpha\beta}, \qquad g_{\alpha 3} = 0, \qquad g_{33} = 1 \qquad (1)$$

where g_{ij}, $a_{\alpha\beta}$, and $\delta_{\alpha\beta}$ denote the components of the spatial and surface metric tensors, and of Kronecker delta, respectively. Partial differentiation (coinciding in this system of coordinates with the covariant one) will be denoted by a comma $(\ )_{,i} \equiv \partial(\ )/\partial x_i$. Throughout the paper, Einsteinian summation convention will be used with Latin indices ranging from 1–3 and Greek indices ranging from 1–2. An index in the brackets "$\langle\ \rangle$" associated with a field quantity identifies its affiliation to the layer of the laminate indicated by that index.

Displacement Representation and Strain Measures

The results obtained in Refs. 13–16 reveal that the first-order transverse shear deformation theory (FSDT) could play an essential role in the accurate prediction of static and dynamic responses of composite flat panels, in general, and of their postbuckling, in particular. In addition to its relative simplicity, the predictions based on this theory could result in an excellent agreement with the ones derived via higher-order theories or via experimental methods[16]. For this reason in the forthcoming development, the geometrically nonlinear theory of imperfect flat composite panels will be modeled within the framework of FSDT. In this light, the 3-D displacement field will be represented as

$$V_\alpha(x_\omega, x_3) = u_\alpha + x_3\psi_\alpha \qquad (2a)$$

$$V_3(x_\omega, x_3) = u_3 \qquad (2b)$$

where $u_\alpha \equiv u_\alpha(x_\omega)$, $u_3 \equiv u_3(x_\omega)$, and $\psi_\alpha \equiv \psi(x_\omega)$ denote the in-plane, transversal, and the angles of rotation of the normals to the midplane, respectively. It is assumed also the existence of an initial, out-of-plane stress-free geometrical imperfection $\mathring{u}_3 \equiv \mathring{u}_3(x_\omega)$. By convention, the transverse deflection $u_3(x_\omega)$ is measured from the imperfect surface.

Within the framework of the Lagrangian formulation and in light of the von Kármán concept, the strain tensor e_{ij} assumes the form

$$2e_{ij} = V_{i,j} + V_{j,i} + V_{3,i}V_{3,j} \qquad (3)$$

Consideration of Eq. (2) into Eq. (3) and incorporation of the stress-free geometric imperfection $\mathring{u}_3$ results in the following expressions for the 3-D strain components:

$$e_{\alpha\beta} = \varepsilon_{\alpha\beta} + x_3\kappa_{\alpha\beta} \qquad (4a)$$

$$e_{\alpha 3} = \varepsilon_{\alpha 3} \qquad (4b)$$

$$e_{33} = 0 \qquad (4c)$$

In Eqs. (4) the two-dimensional (2-D) strain measures assume the form:

$$2\varepsilon_{\alpha\beta} = u_{\alpha,\beta} + u_{\beta,\alpha} + u_{3,\alpha}\,\mathring{u}_{3,\beta} + \mathring{u}_{3,\alpha}u_{3,\beta} + u_{3,\alpha}u_{3,\beta} \qquad (5a)$$

$$2\kappa_{\alpha\beta} = \psi_{\alpha,\beta} + \psi_{\beta,\alpha} \qquad (5b)$$

$$2\varepsilon_{\alpha 3} = \psi_\alpha + u_{3,\alpha} \qquad (5c)$$

Equations of Equilibrium

The 2-D equations of equilibrium of flat composite panels are obtained by taking the nth moments ($n = 0, 1$) of the equations of equilibrium of the 3-D geometrically nonlinear elasticity theory in Lagrangian description[2]:

$$[s_{ij}(\delta_{jr} + V_{j,r})]_{,i} = 0 \qquad (6)$$

where s_{ij} denotes the second Piola-Kirchhoff stress tensor. Moreover, incorporation in Eq. (6) of the effect of geometric imperfection and its simplification in accordance with the von Kármán concept yields the following equations of 2-D equilibrium of the composite plate element:

$$L_{\alpha\beta,\alpha} = 0 \qquad (7a)$$

$$L_{\alpha\beta}(u_{3,\beta} + \mathring{u}_{3,\beta})_{,\alpha} + Q_{\alpha,\alpha} + p_3 = 0 \qquad (7b)$$

$$M_{\alpha\beta,\beta} - Q_\alpha = 0 \qquad (7c)$$

Here $L_{\alpha\beta}$, $M_{\alpha\beta}$, and Q_α defined as

$$(L_{\alpha\beta}, M_{\alpha\beta}) \equiv 2\sum_{k=1}^{m+1} \int_{h_{(k-1)}}^{h_{(k)}} s_{\alpha\beta}(1, x_3)\,\mathrm{d}x_3 \qquad (8a)$$

$$Q_\alpha = 2\sum_{k=1}^{m+1} \int_{h_{(k-1)}}^{h_{(k)}} s_{\alpha 3}\,\mathrm{d}x_3 \qquad (8b)$$

denote the stress resultant, stress couple, and transverse-shear stress resultants, respectively. Equations (7) represent the generalized counterpart of the equations of equilibrium obtained for perfect plates in Ref. 2.

Constitutive Equations

The 3-D constitutive equations associated with an elastic transversely isotropic body (the planes of isotropy being parallel to the plane $x_3 = 0$) are given by[2]

$$s_{\alpha\beta} = \bar{E}_{\alpha\beta\omega\zeta}e_{\omega\zeta}, \qquad s_{\alpha 3} = 2E_{\alpha 3\omega 3}e_{\omega 3} \qquad (9)$$

where

$$\bar{E}_{\alpha\beta\omega\zeta} = \frac{E}{1+\nu}\left[\frac{1}{2}(a_{\alpha\omega}a_{\beta\zeta} + a_{\alpha\zeta}a_{\beta\omega}) + \frac{\nu}{1-\nu}a_{\omega\zeta}a_{\alpha\beta}\right] \qquad (10a)$$

$$E_{\alpha 3\omega 3} = G'a_{\alpha\omega} \qquad (10b)$$

Here E and ν denote Young's modulus and Poisson's ratio in the plane of isotropy, respectively, while G' denotes the shear modulus in the plane normal to the isotropy plane.

Equations (8), in conjunction with Eqs. (9), (10), (4), and (5), yield the 2-D constitutive equations:

$$L_{\alpha\beta} = \tfrac{1}{2}\mathscr{A}_{\alpha\beta\omega\zeta}(u_{\omega,\zeta} + u_{\zeta,\omega} + u_{3,\omega}u_{3,\zeta} + \mathring{u}_{3,\omega}u_{3,\zeta}$$
$$+ u_{3,\omega}\mathring{u}_{3,\zeta}) \qquad (11a)$$

$$M_{\alpha\beta} = \tfrac{1}{2}\mathscr{D}_{\alpha\beta\omega\zeta}(\psi_{\omega,\zeta} + \psi_{\zeta,\omega}) \qquad (11b)$$

$$Q_\alpha = \mathscr{R}_{\alpha 3\omega 3}(\psi_\omega + u_{3,\omega}) \qquad (11c)$$

In Eqs. (11), $\mathscr{A}_{\alpha\beta\omega\zeta}$, $\mathscr{D}_{\alpha\beta\omega\zeta}$, and $\mathscr{R}_{\alpha 3\omega 3}$ denote the stretching, the transverse shear, and the bending rigidities of the transversely isotropic composite structure, respectively. Their expressions are

$$\mathscr{A}_{\alpha\beta\omega\zeta} = 2\left[{}_{\langle m+1\rangle}\bar{E}_{\alpha\beta\omega\zeta}h_{\langle m+1\rangle}\right.$$
$$\left. + \sum_{r=1}^{m} {}_{\langle r\rangle}\bar{E}_{\alpha\beta\omega\zeta}(h_{\langle r\rangle} - h_{\langle r+1\rangle})\right] \qquad (12a)$$

$$\mathscr{D}_{\alpha\beta\omega\zeta} = \frac{2}{3}\left[{}_{\langle m+1\rangle}\bar{E}_{\alpha\beta\omega\zeta}h^3_{\langle m+1\rangle}\right.$$
$$\left. + \sum_{r=1}^{m} {}_{\langle r\rangle}\bar{E}_{\alpha\beta\omega\zeta}(h^3_{\langle r\rangle} - h^3_{\langle r+1\rangle})\right] \qquad (12b)$$

$$\mathfrak{R}_{\alpha 3 \omega 3} = 2K^2 \left[{}_{\langle m+1 \rangle} E_{\alpha 3 \omega 3} h_{\langle m+1 \rangle} \right.$$
$$\left. + \sum_{r=1}^{m} {}_{\langle r \rangle} E_{\alpha 3 \omega 3} (h_{\langle r \rangle} - h_{\langle r+1 \rangle}) \right] \qquad (12c)$$

where K^2 denotes the transverse-shear correction factor. For a single-layered plate,

$$\sum_{r=1}^{m} (\cdot) \to 0 \quad \text{and} \quad h_{\langle m+1 \rangle} \to h/2$$

Governing System

A mixed formulation of the governing equations of geometrically nonlinear imperfect composite flat panels will be given. It represents a generalization to the case of laminated shear-deformable imperfect plates of von Kármán's classical equations. To this end, the ensuing steps will be considered:

1) Expression of stress resultants $L_{\alpha\beta}$ in terms of in-plane strains $\varepsilon_{\alpha\beta}$. Based on Eqs. (10a), (11a), (12a), and (5a) this relationship is

$$L_{\alpha\beta} = b\varepsilon_{\alpha\beta} + c\delta_{\alpha\beta}\varepsilon_{\omega\omega} \qquad (13)$$

wherefrom its inverted counterpart results as

$$\varepsilon_{\alpha\beta} = \tilde{b}L_{\alpha\beta} + \tilde{c}\delta_{\alpha\beta}L_{\omega\omega} \qquad (14)$$

In Eqs. (13) and (14), the coefficients b, c, and their tilded counterparts are given by

$$b = 2\left[\frac{E_{\langle m+1 \rangle} h_{\langle m+1 \rangle}}{1 + \nu_{\langle m+1 \rangle}} + \sum_{r=1}^{m} \frac{E_{\langle r \rangle}(h_{\langle r \rangle} - h_{\langle r+1 \rangle})}{1 + \nu_{\langle r \rangle}} \right] \qquad (15a)$$

$$c = 2\left[\frac{E_{\langle m+1 \rangle} \nu_{\langle m+1 \rangle} h_{\langle m+1 \rangle}}{1 - \nu_{\langle m+1 \rangle}^2} \right.$$
$$\left. + \sum_{r=1}^{m} \frac{E_{\langle r \rangle} \nu_{\langle r \rangle}(h_{\langle r \rangle} - h_{\langle r+1 \rangle})}{1 - \nu_{\langle r \rangle}^2} \right] \qquad (15b)$$

$$\tilde{b} = 1/b, \qquad \tilde{c} = -\frac{c}{b(b + 2c)} \qquad (15c)$$

2) Representation of the stress resultants $L_{\alpha\beta}$ in terms of an Airy stress function $F[\equiv F(x_\omega)]$, allowing one to satisfy identically Eqs. (7a). This results in

$$L_{\alpha\beta} = c_{\alpha\lambda} c_{\beta\omega} F_{,\lambda\omega} \qquad (16)$$

where $c_{\alpha\beta}$ denotes the permutation symbol.

3) Deduction of the compatibility equation (CE). To this end, elimination of u_α in Eq. (5a) yields the CE:

$$c_{\alpha\pi} c_{\beta\lambda} [\varepsilon_{\alpha\beta,\pi\lambda} + \tfrac{1}{2} u_{3,\alpha\beta} u_{3,\pi\lambda} + \tfrac{1}{2} \mathring{u}_{3,\pi\lambda} u_{3,\alpha\beta}$$
$$+ \tfrac{1}{2} u_{3,\pi\lambda} \mathring{u}_{3,\alpha\beta}] = 0 \qquad (17)$$

4) Substitution of Eqs. (11) [considered in conjunction with Eqs. (12), (14), and (16)] in Eqs. (7b), (7c), and (17). This yields the following system of partial differential equations in terms of the unknown functions F, u_3, and ψ_α:

$$c_{\alpha\lambda} c_{\beta\mu} F_{,\lambda\mu}(u_{3,\alpha\beta} + \mathring{u}_{3,\alpha\beta}) + S(\psi_{\omega,\omega} + u_{3,\omega\omega}) + p_3 = 0 \qquad (18a)$$

$$B\psi_{\omega,\omega\alpha} + C\psi_{\alpha,\omega\omega} - S(\psi_\alpha + u_{3,\alpha}) = 0 \qquad (18b)$$

$$(\tilde{b} + \tilde{c})F_{,\lambda\lambda\omega\omega} + \tfrac{1}{2}(u_{3,\lambda\lambda} u_{3,\zeta\zeta} - u_{3,\lambda\zeta} u_{3,\lambda\zeta})$$
$$+ (\mathring{u}_{3,\lambda\lambda} u_{3,\zeta\zeta} - \mathring{u}_{3,\lambda\zeta} u_{3,\lambda\zeta}) = 0 \qquad (18c)$$

In these equations $(\cdot)_{,\lambda\lambda}$ $[\equiv \nabla^2(\cdot) = \Delta(\cdot)]$ and $(\cdot)_{,\lambda\lambda\omega\omega}$ $[\equiv \nabla^2\nabla^2(\cdot)]$ denote Laplace and biharmonic operators, respectively, while the rigidity quantities B, C, and S are defined as

$$B \equiv \frac{1}{3}\left[\overline{E}_{\langle m+1 \rangle}(1 + \nu_{\langle m+1 \rangle})h_{\langle m+1 \rangle}^3 \right.$$
$$\left. + \sum_{r=1}^{m} \overline{E}_{\langle r \rangle}(1 + \nu_{\langle r \rangle})(h_{\langle r \rangle}^3 - h_{\langle r+1 \rangle}^3) \right] \qquad (19a)$$

$$C \equiv \frac{1}{3}\left[\overline{E}_{\langle m+1 \rangle}(1 - \nu_{\langle m+1 \rangle})h_{\langle m+1 \rangle}^3 \right.$$
$$\left. + \sum_{r=1}^{m} \overline{E}_{\langle r \rangle}(1 - \nu_{\langle r \rangle})(h_{\langle r \rangle}^3 - h_{\langle r+1 \rangle}^3) \right] \qquad (19b)$$

$$S \equiv 2G'_{\langle m+1 \rangle} h_{\langle m+1 \rangle} + 2\sum_{r=1}^{m} G'_{\langle r \rangle}(h_{\langle r \rangle} - h_{\langle r+1 \rangle}) \qquad (19c)$$

where $\overline{E} \equiv E(1 - \nu^2)$.

The final step yielding the system of Eqs. (18) to a form that could be viewed as a generalization of von Kármán classical equations consists of expressing ψ_α in Eq. (18a) in terms of a potential function $\phi[\equiv \phi(x_\omega)]$, as

$$\psi_\alpha = -\frac{B + C}{S} u_{3,\omega\omega\alpha} + \frac{1}{S} c_{\alpha\mu}\phi_{,\mu} - u_{3,\alpha}$$
$$- \frac{B + C}{S^2} p_{3,\alpha} - \frac{B + C}{S^2} [L_{\omega\zeta}(u_{3,\omega\zeta} + \mathring{u}_{3,\omega\zeta})]_{,\alpha} \qquad (20)$$

Substitution of Eq. (20) into Eqs. (18a) and (18b) yields

$$D\nabla^4 u_3 - c_{\alpha\lambda} c_{\beta\omega} F_{,\lambda\omega}(u_{3,\alpha\beta} + \mathring{u}_{3,\alpha\beta})$$
$$+ \frac{B + C}{S} c_{\alpha\lambda} c_{\beta\omega} \nabla^2[F_{,\lambda\omega}(u_{3,\alpha\beta} + \mathring{u}_{3,\alpha\beta})] - p_3$$
$$+ \frac{B + C}{S} \nabla^2 p_3 = 0 \qquad (21)$$

and

$$\phi - \frac{C}{S}\Delta\phi = 0 \qquad (22)$$

while replacement of $\varepsilon_{\alpha\beta}$ in Eq. (17) by Eq. (14) considered in conjunction with Eq. (16) results in the third governing equation:

$$(\tilde{b} + \tilde{c})\nabla^4 F + (u_{3,11} u_{3,22} - (u_{3,12})^2 + u_{3,11}\mathring{u}_{3,22}$$
$$+ u_{3,22}\mathring{u}_{3,11} - 2\mathring{u}_{3,12} u_{3,12}) = 0 \qquad (23)$$

In Eq. (21),

$$D \equiv \frac{2}{3}\left[\overline{E}_{\langle m+1 \rangle} h_{\langle m+1 \rangle}^3 + \sum_{r=1}^{m} \overline{E}_{\langle r \rangle}(h_{\langle r \rangle}^3 - h_{\langle r+1 \rangle}^3) \right] \qquad (24)$$

denotes the bending rigidity.

Equations (21–23) represent the counterpart of classical von Kármán large-deflection plate theory extended to transversely isotropic composite imperfect flat panels. A special form of these equations could be found in Refs. 13 and 17. It may easily be seen that for $G'_{\langle k \rangle} \to \infty$ (yielding $S \to \infty$), Eqs. (21–23) reduce to the familiar von Kármán equations.

Linearization of Eqs. (21–23) yields the equations obtained by Reissner[18,19] (and reobtained in a more general framework through an alternative procedure in Refs. 20 and 21; see also Ref. 2). It should be remarked that Eq. (22) (of a Helmholtz-

type, whose solution has the character of a boundary-layer solution) is decoupled from the remaining two governing equations [i.e., Eqs. (21) and (23)]. However, the function ϕ intervenes in a coupled form in the boundary conditions.

Furthermore, for simply supported boundary conditions, it could be shown (see Ref. 13) that the function ϕ could be decoupled in the boundary conditions (BCs) to result as

$$\partial\phi/\partial n = 0 \tag{25}$$

at a boundary whose outward normal to the contour is n = ne_n. Since the governing equation for ϕ is homogeneous, the solution of Eq. (22), in conjunction with the BC, Eq. (25), is identically zero everywhere throughout the domain of the plate.

In such a case, Eq. (22) could exactly be discarded and consequently the system of governing equations reduces to Eqs. (21) and (23). This entails a reduction of the order of governing equations from ten to eight and, as a result, the number of BCs reduces from five to four. For the case of perfect plates the BCs have been displayed in Ref. 13 while for the linear theory in Ref. 22.

Postbuckling Behavior of Compressed Rectangular Imperfect Panels

Boundary Conditions

In what follows, the static postbuckling behavior of simply supported (SS) composite rectangular ($l_1 \times l_2$) flat panels will be analyzed. The in-plane rectangular axes x_α will be selected to coincide with the panel edges. It is assumed that during the postbuckling process no delamination may occur. Consider that the panel is subjected to a system of uniform in-plane biaxial compressive edge loads $\tilde{L}_1$ and $\tilde{L}_2$. Within this problem the terms associated with the transversal load p_3 should be discarded. Depending upon the in-plane behavior at the edges, two cases, referred to as cases 1 and 2, will be considered.

Case 1: The edges are SS and freely movable (in the in-plane direction). In addition the panel is subjected to biaxial compressive edge loads $\tilde{L}_1$ and $\tilde{L}_2$. As a result, as it may easily be shown, the resulting system of governing equations admits the BCs:

At $x_1 = 0, l_1$:

$$\underline{u_3 = 0}, \qquad Du_{3,11} + \frac{B+C}{S} L_{11}(u_{3,11} + \mathring{u}_{3,11}) = 0$$

$$\underline{L_{12} = 0}, \qquad \text{and} \qquad L_{11} = -\tilde{L}_1 \tag{26}$$

At $x_2 = 0, l_2$:

$$\underline{u_3 = 0}, \qquad Du_{3,22} + \frac{B+C}{S} L_{22}(u_{3,22} + \mathring{u}_{3,22}) = 0$$

$$\underline{L_{21} = 0}, \qquad \text{and} \qquad L_{22} = -\tilde{L}_2$$

Case 2: The edges are SS. Uniaxial compressive edge loads are applied in the direction of the x_1 coordinate. The edges $x_1 = 0, l_1$ are considered freely movable (in the in-plane direction), the remaining two edges being unloaded and immovable. For this case the BCs become

At $x_1 = 0, l_1$:

$$\underline{u_3 = 0}, \qquad Du_{3,11} + \frac{B+C}{S} L_{11}(u_{3,11} + \mathring{u}_{3,11}) = 0$$

$$\underline{L_{12} = 0}, \qquad \text{and} \qquad L_{11} = -\tilde{L}_1 \tag{27}$$

At $x_2 = 0, l_2$:

$$\underline{u_3 = 0}, \qquad Du_{3,22} + \frac{B+C}{S} L_{22}(u_{3,22} + \mathring{u}_{3,22}) = 0$$

$$\underline{u_2 = 0}, \qquad \text{and} \qquad L_{21} = 0$$

In Eqs. (26) and (27) the underlined terms are associated with the out-of-plane BCs.

Postbuckling Solution

By simple inspection it may be seen that expressing

$$\begin{Bmatrix} u_3 \\ \mathring{u}_3 \end{Bmatrix} = \begin{Bmatrix} f_{mn} \\ \mathring{f}_{mn} \end{Bmatrix} \sin\lambda_m x_1 \sin\mu_n x_2$$

$$\lambda_m \equiv m\pi/l_1, \qquad \mu_n = n\pi/l_2 \tag{28}$$

(where the shape of geometric imperfection is similar to the one of the buckling mode) the out-of-plane BCs are identically fulfilled. The in-plane BCs will be satisfied on an average. To this end, the potential function F is represented as

$$F(x_1, x_2) = F_1(x_1, x_2) - \tfrac{1}{2}[(x_2)^2 \tilde{L}_1 + (x_1)^2 \tilde{L}_2] \tag{29}$$

Here $F_1(x_1, x_2)$ is a particular solution of Eq. (23), [determined in conjunction with Eq. (28)], while $\tilde{L}_1$ and $\tilde{L}_2$ denote the in-plane normal edge loads (positive in compression). Upon imposing the conditions that concern the function F_1,

$$\int_0^{l_2} F_{1,22}\big|_{x_1=0} \, dx_2 = \int_0^{l_2} F_{1,22}\big|_{x_1=l_1} \, dx_2 = 0 \tag{30a}$$

$$\int_0^{l_2} F_{1,11}\big|_{x_2=0} \, dx_1 = \int_0^{l_2} F_{1,11}\big|_{x_2=l_2} \, dx_1 = 0 \tag{30b}$$

$$\int_0^{l_2} F_{1,12}\big|_{x_1=0} \, dx_2 = \int_0^{l_2} F_{1,12}\big|_{x_1=l_1} \, dx_2 = 0 \tag{30c}$$

$$\int_0^{l_1} F_{1,12}\big|_{x_2=0} \, dx_1 = \int_0^{l_1} F_{1,12}\big|_{x_2=l_2} \, dx_1 = 0 \tag{30d}$$

the parameters $\tilde{L}_1$ and $\tilde{L}_2$ acquire the meaning of average in-plane normal edge loads

$$-\tilde{L}_1 = \frac{1}{l_2} \int_0^{l_2} F_{,22}\big|_{x_1=0,l_1} \, dx_2 \tag{31a}$$

$$-\tilde{L}_2 = \frac{1}{l_1} \int_0^{l_1} F_{,11}\big|_{x_2=0,l_2} \, dx_1 \tag{31b}$$

In the case of the plate loaded in the direction of the x_1 coordinate only (that is of the case 2), the condition for the immovable edges $x_2 = 0, l_2$ may be expressed, on an average, as[2,23]

$$\int_0^{l_1}\int_0^{l_2} u_{2,2} \, dx_1 \, dx_2 = 0 \tag{32}$$

By virtue of Eqs. (14), (5a), and (16), Eq. (32) results in

$$\int_0^{l_1}\int_0^{l_2} [(\tilde{b} + \tilde{c})F_{,11} + \tilde{c}F_{,22} - \tfrac{1}{2}(u_{3,2})^2$$

$$- u_{3,2}\mathring{u}_{3,2}] \, dx_1 \, dx_2 = 0 \tag{33}$$

This equation [considered in conjunction with Eqs. (28) and (29)] provides the fictitious edge load $\tilde{L}_2$ for which the edges $x_2 = 0, l_2$ should remain immovable.

For the present case, $F_1(x_1, x_2)$ is

$$F_1(x_1, x_2) = A_1 \cos 2\lambda_m x_1 + A_2 \cos 2\mu_n x_2 \qquad (34)$$

where

$$A_1 \equiv \frac{(f_{mn}^2 + 2f_{mn}\overset{\circ}{f}_{mn})}{32(\bar{b} + \bar{c})} \frac{\mu_n^2}{\lambda_m^2}$$

$$A_2 \equiv \frac{(f_{mn}^2 + 2f_{mn}\overset{\circ}{f}_{mn})}{32(\bar{b} + \bar{c})} \frac{\lambda_m^2}{\mu_n^2} \qquad \overset{\displaystyle\sum'}{{}_{m,n}} \qquad (35)$$

while $\overset{\displaystyle\sum'}{{}_{m,n}}$ indicates that in the equations accompanied by this sign no summation with respect to indexes m and n is involved. The final step consists of application of Galerkin's method to the Eq. (21). To this end, substitution of u_3, $\overset{\circ}{u}_3$, and F expressed, respectively, by Eqs. (28), (34), and (29) into Eq. (21), followed by its multiplication by $\sin\lambda_p x_1 \sin\mu_s x_2$ and integration of the obtained equation over the panel area, yields

$$\tilde{L}_1 + \frac{\gamma_1}{\gamma_2}\tilde{L}_2$$

$$= \left\{ \frac{\pi^2}{\Gamma^2} + \frac{\Lambda\pi^2 h^2(\delta_{mn}^2 + 3\delta_{mn}\overset{\circ}{\delta}_{mn} + 2\overset{\circ}{\delta}_{mn}^2)}{32D(m^2 + n^2\phi^2)^2\Gamma^2} \gamma_3 \right\}$$

$$\times \frac{\delta_{mn}}{\delta_{mn} + \overset{\circ}{\delta}_{mn}}, \qquad \overset{\displaystyle\sum'}{{}_{m,n}} \qquad (36)$$

Equation (36), obtained for case 1, constitutes an explicit relationship between the average applied compressive loads and the maximum lateral deflection subsequent to the onset of buckling. Moreover, consideration in Eq. (36) of $\overset{\circ}{\delta}_{mn} = 0$, followed by its linearization, yields the (nondimensional) buckling load in biaxial compression of shear deformable composite plates. In the case of immovable edges, $x_2 = 0$, l_2, employment of Eqs. (28) and (34) in Eq. (33) yields

$$\tilde{L}_2 = -\frac{1}{\bar{b} + \bar{c}}\left\{ \bar{c}\,\tilde{L}_1 + \frac{1}{8}\frac{n^2\phi^2 h^2}{D}\delta_{mn}^2 \right.$$

$$\left. + \frac{1}{4}\frac{n^2\phi^2 h^2}{D}\delta_{mn}\overset{\circ}{\delta}_{mn} \right\}, \qquad \overset{\displaystyle\sum'}{{}_{m,n}} \qquad (37)$$
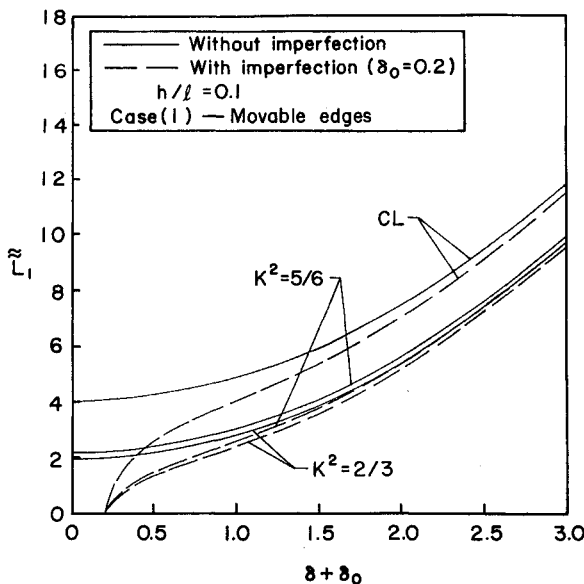
Fig. 2   Postbuckling in uniaxial compression of a square composite plate (case 1) with movable edges. Comparison between the classical and refined theories as well as between the initially perfect and imperfect flat geometries.
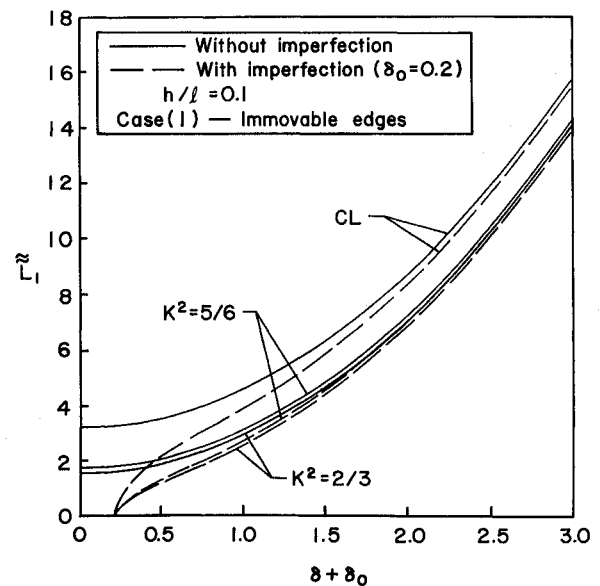
Substitution of Eq. (37) into Eq. (36) results in the equation governing the postbuckling for immovable edge conditions.

In Eqs. (36) and (37), the newly introduced notations are

$$\gamma_1 \equiv \frac{n^2 l_1^2 \phi^2}{\pi^2} + \frac{B + C}{S}(n^4\phi^4 + m^2 n^2\phi^2) \qquad (38a)$$

$$\gamma_2 \equiv \frac{m^2 l_1^2}{\pi^2} + \frac{B + C}{S}(m^4 + m^2 n^2\phi^2) \qquad (38b)$$

$$\gamma_3 \equiv m^4 + n^4\phi^4 + \frac{B + C}{S}\frac{\pi^2}{l_1^2}$$

$$\times (n^6\phi^6 + n^4 m^2\phi^4 + n^2 m^4\phi^2 + m^6) \qquad (38c)$$

$$\{\delta_{mn}, \overset{\circ}{\delta}_{mn}\} \equiv \{f_{mn}, \overset{\circ}{f}_{mn}\}/h \qquad (38d)$$

$$\{\tilde{L}_1, \tilde{L}_2\} \equiv \{(\bar{L}_1, \bar{L}_2)l_1^2/\pi^2 D\} \qquad (38e)$$

$$\Lambda \equiv 2b(b + 2c)/D(b + c) \qquad (38f)$$

$$\Gamma^2 \equiv \pi^2\left[m^2 + \frac{\pi^2}{l_1^2}\frac{B + C}{S}(m^4 + m^2 n^2\phi^2) \right]$$

$$/(m^2 + n^2\phi^2)^2 \qquad (38g)$$

where $\phi = l_1/l_2$.

The Eq. (36) and its immovable counterpart [obtained in conjunction with Eq. (37)] determine in closed form the behavior of composite laminated plates subsequent to the onset of buckling. The Kirchhoffean counterpart of the above-mentioned equations may be obtained by letting $G'_{(k)} \to \infty$ in the expression of the rigidity S. From both Eq. (36) and its associated immovable counterpart, it may be remarked that when $\overset{\circ}{\delta} = 0$ the postbuckling behavior could be expressed generically as

$$\bar{L}_1/(\bar{L}_1)_{cr} = 1 + \lambda\delta^2 \qquad (39)$$

where $\bar{L}_1/(\bar{L}_1)_{cr}$ is the ratio of the applied load (nondimensional) to the buckling load of the associated perfect panel while λ is a coefficient, (referred to as Koiter's postbuckling parameter). This coefficient incorporates the effects of transverse shear deformation, geometry of the panel, type of load-

Fig. 3   Postbuckling in uniaxial compression of a square composite plate (case 1) with immovable edges. Comparison between the classical and refined theories as well as between the initially perfect and imperfect flat geometries.
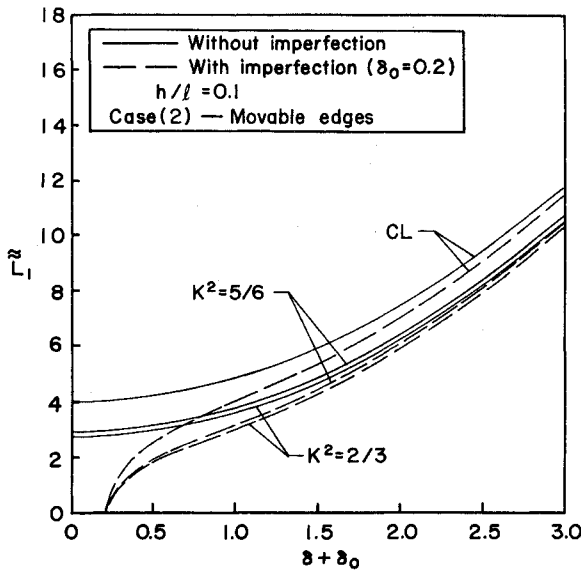
Fig. 4 Postbuckling in uniaxial compression of a square composite plate (case 2) with movable edges. Comparison between the classical and refined theories as well as between the initially perfect and imperfect flat geometries.
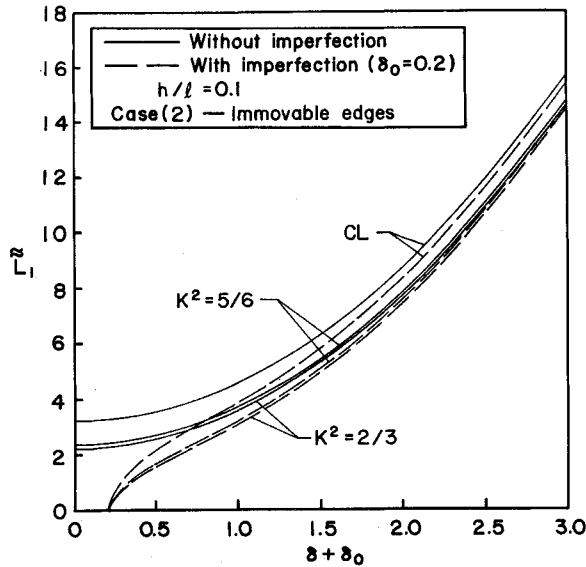
Fig. 5 Postbuckling in uniaxial compression of a square composite plate (case 2) with immovable edges. Comparison between the classical and refined theories as well as between the initially perfect and imperfect flat geometries.

ing, prebuckling behavior, etc. From both Eq. (36) and its immovable counterpart, it may easily be seen that for the case of flat panels, λ turns out to be a positive quantity. As a result, $L_1/(L_1)_{cr}$ is larger than unity, thus predicting that the perfect (and imperfect flat structures) can support loads in excess of the buckling load. This qualitative result will be supplemented by several numerical ones.

Numerical Illustrations

The numerical illustrations concern the cases of single- and three-layered composite square plates. Regarding the latter case, two instances labeled as case 1 and case 2 are considered, namely:

Case 1:

$$\frac{E_{(2)}}{G'_{(2)}} = 10, \qquad \frac{E_{(1)}}{G'_{(1)}}\left(\equiv \frac{E_{(3)}}{G'_{(3)}}\right) = 30$$

$$\frac{E_{(1)}}{E_{(2)}}\left(\equiv \frac{E_{(3)}}{E_{(2)}}\right) = 10 \qquad\qquad (40a)$$

Case 2:

$$\frac{E_{(2)}}{G'_{(2)}} = 30, \qquad \frac{E_{(1)}}{G'_{(1)}}\left(\equiv \frac{E_{(3)}}{G'_{(3)}}\right) = 10$$

$$\frac{E_{(1)}}{E_{(2)}}\left(\equiv \frac{E_{(3)}}{E_{(2)}}\right) = 10 \qquad\qquad (40b)$$

For both cases,

$$\nu_{(1)} = \nu_{(2)} = \nu_{(3)} = 0.25$$

At this point it should be emphasized that due to the character of FSDT plate theory, wherein s_{33} is not involved, the additional coefficients ν' and E' (i.e., Poisson's ratio and Young's modulus in transverse direction) do not intervene[2].
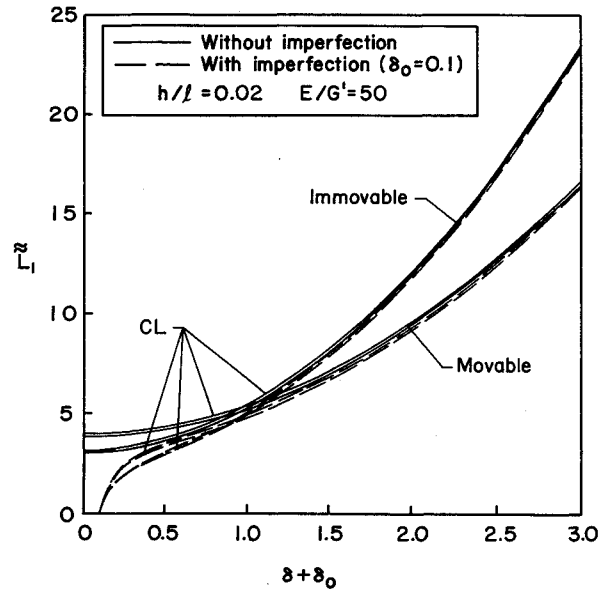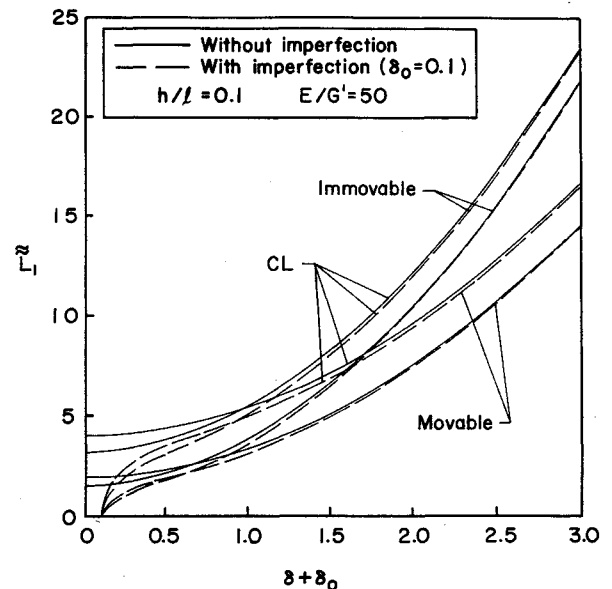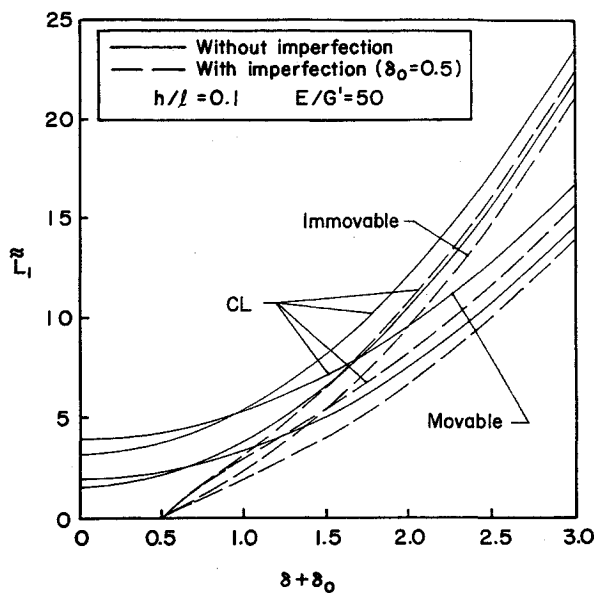

Fig. 6 Postbuckling behavior of a single-layered square plate with movable and immovable edges. Comparison between the classical and refined theories as well as between the initially perfect and imperfect flat geometries.

Fig. 7 Postbuckling behavior of a single-layered square plate with movable and immovable edges. Comparison between the classical and refined theories as well as between the initially perfect and imperfect flat geometries.

Fig. 8 Postbuckling behavior of a single-layered square plate with movable and immovable edges. Comparison between the classical and refined theories as well as between the initially perfect and imperfect flat geometries.
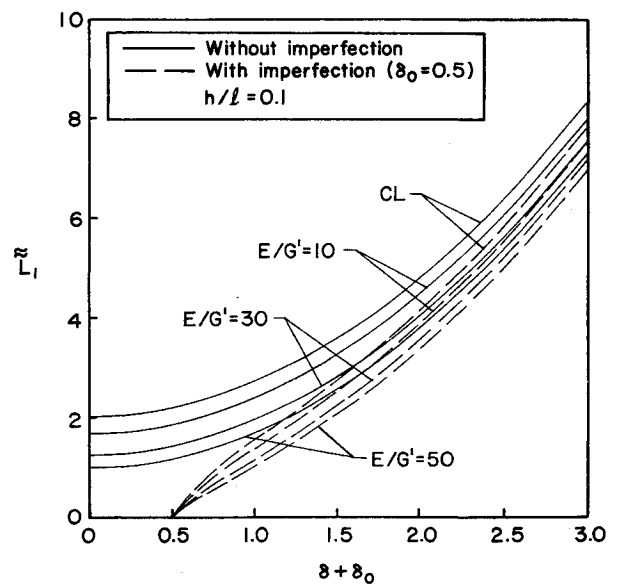

Fig. 10 Postbuckling behavior of a single-layered square plate with movable edges under biaxial compression. Influence of the initial imperfection as well as of transverse-shear flexibility effects.
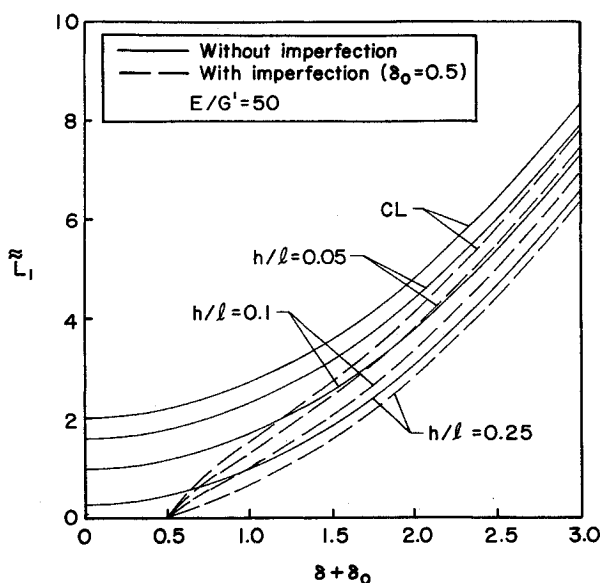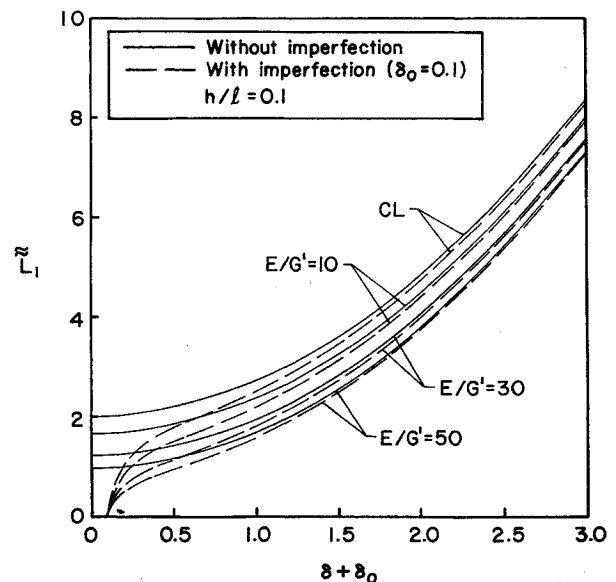

Fig. 9 Postbuckling behavior of a single-layered square plate with movable edges under biaxial compression. Influence of the thickness ratio, initial imperfection, as well as of transverse-shear flexibility effects.

Fig. 11 Postbuckling behavior of a single-layered square plate with movable edges under biaxial compression. Influence of the initial imperfection as well as of transverse-shear flexibility effects.

In addition, it is assumed that the midlayer of the three-layered plate is two times thicker than the external ones [implying that $h_{(1)}/h(= h_{(3)}/h) = 0.5$ and $h_{(2)}/h = 0.25$; see Fig. 1].

Figures 2–5 and Figs. 6–11 display the postbuckling behavior of three-layered composite and single-layered geometrically perfect and imperfect square ($l_1 = l_2 \equiv l$) plates, respectively. Within their framework, the dependence of the nondimensional compressive load parameter $\tilde{L}_1$ vs the total nondimensional deflection

$$\delta + \delta_0 \ (= f_{11}/h + \mathring{f}_{11}/h)$$

of the central point of the plate was depicted. Curves for several different values of the ratios E/G', h/l, the initial imperfection δ_0, transverse-shear correction factor K^2, as well as for the cases of freely movable and immovable edges $x_2 = 0, l_2$, are presented.

Throughout the numerical illustrations, unless otherwise stated, a shear correction factor $K^2 = \frac{5}{6}$ was used. In Figs. 2–11, the points on the axis of coordinates (occurring for the perfect panels) correspond to their associated buckling bifurcation loads.

Conclusions

A shear-deformable theory of geometrically nonlinear composite plates symmetrically laminated of transversely isotropic material layers incorporating the effect of initial geometric imperfection was developed. The associated governing equations have been recast in a form representing a generalization of both Reissner's linear plate theory[18,19] and of some of the previous author's results[2,20,21] as well as of classical von Kármán large-deflection theory of geometrically perfect flat panels. The obtained equations are used to analyze the postbuckling of simply supported shear-deformable plates.

The numerical results displayed in Figs. 2–11 allow one to conclude the following:

1) The geometrically perfect flat panels (both composite and single-layered) are capable of carrying increased compressive loads well beyond the instant at which buckling occurs. However, as the plate becomes weaker in transverse shear, i.e., when E/G' increases (see Figs. 10 and 11), severe reductions of its load-carrying capacity as compared to its rigid-in-transverse shear counterpart (corresponding to $E/G' \to 0$) are manifested. In the case of a three-layered composite plate (see Figs. 2–5), the increase of transverse shear flexibility (TSF) of the face layers (case 1) yields a stronger reduction of their postbuckling carrying capacity as compared to the case when the increase of TSF is manifested in the core layer (case 2), only.

2) The bending of initially geometric imperfect panels starts at once as the compressive load is applied (see Figs. 2–11). The deflections start to increase slowly, and then, in the vicinity of the buckling bifurcation of their perfect plate counterparts, a marked increase in the bending is experienced. As it may be remarked from the same figures, with the increase of the initial geometric imperfection, in the region of small deflections a significant reduction of load-carrying capacity of the panel is experienced. However, as the deflections increase in magnitude, the curves of the initially imperfect plate approach the ones of their perfect counterparts. This reverts to the conclusion that the load-carrying capacity of flat panels is insensitive to imperfections in the extended postbuckling range. These conclusions are valid for both classical and shear-deformable composite and single-layered flat panels. Moreover, in the case of thin plates or when the plate becomes less transverse shear deformable, the results reveal that the difference in the postbuckling behavior of shear-deformable and infinitely rigid-in-transverse-shear plates declines, and sometimes (see Fig. 6) it becomes almost immaterial. In the latter case the classical plate theory could be successfully employed in the postbuckling analysis. For this instance, the present results fully agree with the ones in Ref. 24 developed for the classical plate theory.

3) The classical Kirchhoff's plate model provides results inadvertently overestimating the true ones, which, for non-thin plates and when the plate material exhibits high transverse shear flexibility properties, are independent of the ratios E/G' characterizing the actual plate.

4) As seen from Figs. 2–8, the in-plane boundary conditions have a significant effect both in the case of shear-deformable and of transversely rigid plates (for this latter case see Refs. 2 and 24). Even though the buckling bifurcation is slightly reduced, the constraint introduced by the immovable edge conditions has a significant beneficial influence on the postbuckling behavior of both perfect and imperfect plates.

5) Figures 2–5 for laminated composite panels reveal that consideration of $K^2 = \frac{2}{3}$ as opposed to $K^2 = \frac{5}{6}$ yields the most conservative results from the postbuckling point of view, for both perfect and imperfect panels. However, for single-layered perfect plates the results obtained in Ref. 13 reveal that shear correction factor $K^2 = \frac{5}{6}$ provides results in excellent agreement with the ones predicted within the higher-order plate theory.

6) With the increase of the thickness ratio h/l, the postbuckling based on shear-deformable plate theory (see Fig. 9) shows a deterioration of the load-carrying capacity as compared to its classical counterpart. Moreover, when using the load parameter $\bar{L}_1$ [see Eq. (38e)], the postbuckling predictions based on the classical theory appear independent on h/l, as opposed to the case when the predictions are based on the shear-deformable theory.

Finally, it should be remembered that the present geometrically nonlinear plate theory is based on von Kármán's partially nonlinear strain-displacement relationship, Eq. (3), implying the small finite-deflection approximation[25]. Improved predictions, especially in the deep postbuckling range,

could be obtained by relaxing this approximation. Such improved approximations have been considered recently in a number of papers (e.g., Refs. 26–29). In any case, although the displayed results reveal that the panel is capable to carry compressive loads several times larger than the associated buckling ones, the ultimate loads should be determined by using a failure analysis (see e.g., Refs. 10 and 30).

References

[1]Budiansky, B., "Theory of Buckling and Post-Buckling Behavior of Elastic Structures," *Advances in Applied Mechanics*, Vol. 14, edited by C.-S. Yih, Academic, New York, 1974, pp. 1–65.

[2]Librescu, L., *Elasto-Statics and Kinetics of Anisotropic and Heterogeneous Shell-Type Structures*, Noordhoff International, Leyden, The Netherlands, 1975, Chaps. 3, 4.

[3]Hutchinson, J. W., and Koiter, W. T., "Postbuckling Theory," *Applied Mechanics Review*, Vol. 23, 1970, pp. 1353–1366.

[4]Esslinger, M., and Geier, B., "Postbuckling Behavior of Structures," Courses and Lectures No. 236, International Center for Mechanical Sciences, CISM, Springer-Verlag, Vienna, 1975.

[5]Kapania, R. K., and Yang, T. Y., "Buckling, Postbuckling and Nonlinear Vibrations of Imperfect Plates," *AIAA Journal*, Vol. 25, No. 10, 1987, pp. 1338–1346.

[6]Chia, C. Y., "Geometrically Nonlinear Behavior of Composite Plates: A Review," *Applied Mechanics Review*, Vol. 41, No. 12, 1988, pp. 439–450.

[7]Chia, C. Y., *Nonlinear Analysis of Plates*, McGraw-Hill, New York, 1980.

[8]Leissa, A. W., "Buckling of Laminated Composite Plates and Shell Panels," Air Force Wright Aeronautical Lab., Wright-Patterson AFB, AFWAL-TR-85-3069, June 1985.

[9]Bushnell, D., "Computerized Buckling Analysis of Shells," Martinus Nijhoff, Dordrecht, The Netherlands, 1985.

[10]Noor, A. K., Starnes, J. H., Jr., and Waters, W. A., Jr., "Numerical and Experimental Simulations of the Postbuckling Response of Laminated Anisotropic Panels," *Proceedings of the AIAA/ASME/ASCE/AHS/ASC 31st Structures, Structural Dynamics and Materials Conference*, AIAA, Washington, DC, April 1990.

[11]Vinson, J. R., and Chou, T. W., *Composite Materials and Their Use in Structures*, Wiley, New York, 1974.

[12]Garber, A. M., "Pyrolitic Materials for Thermal Protection Systems," *Aerospace Engineering*, Jan. 1963, pp. 126–137.

[13]Librescu, L., and Stein, M., "A Geometrically Nonlinear Theory of Transversely-Isotropic Laminated Composite Plates and Its Use in the Postbuckling Analysis, *Thin Walled Structures*," Special Issue on *Aeronautical Structures*, Vol. 11, 1991, pp. 117–201.

[14]Bhimaraddi, A., "Non-Linear Free Vibration Analysis of Composite Plates with Initial Imperfections and In-Plane Loading," *International Journal of Solids and Structures*, Vol. 25, No. 1, 1989, pp. 34–43.

[15]Noor, A. K., and Burton, W. S., "Assessment of Shear Deformation Theories for Multilayered Composite Plates," *Applied Mechanics Review*, Vol. 42, No. 1, 1989, pp. 1–12.

[16]Minguet, P. J., Dugundji, J., and Lagace, P., "Postbuckling Behavior of Laminated Plates Using a Direct Energy-Minimization Technique," *AIAA Journal*, Vol. 27, No. 12, 1989, pp. 1785–1792.

[17]Reissner, E., "On Small Finite Deflections of Shear Deformable Elastic Plates," *Computer Methods in Applied Mechanics and Engineering*, Vol. 59, 1986, pp. 227–233.

[18]Reissner, E., "On Bending of Elastic Plates," *Quarterly Applied Mathematics*, Vol. 5, No. 1, 1947, pp. 55–68.

[19]Reissner, E., "Reflections on the Theory of Elastic Plates," *Applied Mechanics Review*, Vol. 38, No. 11, 1985, pp. 1453–1464.

[20]Librescu, L., "Sur les Equations de la Theorie Lineaire des Plaques Elastiques Anisotropes," *Comptes Rendus l'Academie des Sciences Paris*, Vol. 267, Sept. 1968, pp. 443–446.

[21]Librescu, L., and Reddy, J. N., "A Few Remarks Concerning Several Refined Theories of Anisotropic Composite Laminated Plates," *International Journal of Engineering Science*, Vol. 27, No. 5, 1989, pp. 515–527.

[22]Pelech, B. L., "Generalized Theory of Shells," L'vov, Visha Skola,

1978, pp. 108–110 (in Russian).

[23]Librescu, L., "Aeroelastic Stability of Orthotropic Heterogeneous Thin Panels in the Vicinity of the Flutter Critical Boundary," *Journal de Mécanique*, Pt. I, 4, 1, 1965, pp. 51–76; Pt. II, 6, 1, 1967, pp. 133–152.

[24]Ilanko, S., and Dickinson, S. M., "The Vibration and Post-Buckling of Geometrically Imperfect, Simply Supported, Rectangular Plates Under Uni-Axial Loading, Part I. Theoretical Approach," *Journal of Sound and Vibration*, Vol. 118, No. 2, 1987, pp. 313–336.

[25]Koiter, W. T., "On the Nonlinear Theory of Thin Elastic Shells," *Proc. Konink. Ned. Akad. Wetensch. Ser. B*, Vol. 69, 1966, pp. 1–54.

[26]Librescu, L., "Refined Geometrically Nonlinear Theories of Anisotropic Laminated Shells," *Quarterly Applied Mathematics*, Vol. 45, No. 1, 1987, pp. 1–22.

[27]Librescu, L., and Schmidt, R., "Refined Theories of Elastic Anisotropic Shells Accounting for Small Strains and Moderate Rotations," *International Journal of Nonlinear Mechanics*, Vol. 23, No. 3, 1988, pp. 217–229.

[28]Reddy, J. N., "A Small Strain and Moderate Rotation Theory of Laminated Anisotropic Plates," *Journal Applied Mechanics*, Vol. 54, Sept. 1987, pp. 623–626.

[29]Dennis, S. T., and Palazotto, A. N., "Large Displacement and Rotational Formulation for Laminated Shells Including Parabolic Transverse Shear," *International Journal of Nonlinear Mechanics*, Vol. 25, No. 1, 1990, pp. 67–86.

[30]Starnes, J. H., Jr., and Rouse, M., "Postbuckling and Failure Characteristics of Selected Flat Rectangular Graphite-Epoxy Plates Loaded in Compression," *Proceedings of the AIAA/ASME/ASCE/AHS 22nd Structures, Structural Dynamics and Materials Conference*, AIAA, New York, April 1981.